Experimental investigation of the Rayleigh–Bénard convection in a yield stress fluid

Zineddine Kebiche, Cathy Castelain, Teodor Burghelea

Experimental investigation of the Rayleigh-Bénard convection in a yield stress fluid.

Zineddine Kebiche, Teodor Burghelea, Cathy Castelain

Cathy.Castelain@univ-nantes.fr

LUNAM Université, Université de Nantes, CNRS, Laboratoire de Thermocinétique, UMR 6607, La Chantrerie, Rue Christian Pauc, B.P. 50609, F-44306 Nantes Cedex 3, France

Abstract

An experimental study of the Rayleigh-Bénard convection in a yield stress fluid (Carbopol® 980) uniformly heated from below in a rectangular cavity with high aspect ratio is presented. By combined integral measurements of the temperature difference between two parallel plates and the local flow velocity within a wide range of heating powers P two distinct regimes are observed. For heating powers smaller then a critical value P_c a purely conductive regime is observed. A gradual increase of the heating power beyond this onset reveals a convective regime manifested through a nonlinear dependence of the temperature difference between plates on the heating power. Simultaneously with this, local measurements of the flow fields reveal a nonlinear increase of the roll pattern amplitude. Regardless the concentration of Carbopol® and in spite of a significant shear thinning behaviour, the Rayleigh-Bénard convection in the Carbopol® gel is found to emerge as an imperfect bifurcation that can be correctly modelled by the Landau theory of phase transitions. A critical slowing down phenomenon is observed corresponding to the onset of convection. The scaling laws of the convective onset P_c and of the corresponding temperature difference ΔT_c with the relevant material properties are discussed. The onset of the instability can be described in terms of a critical yield number rather than in terms of a critical Rayleigh number. The paper closes with a comparison of our findings with existing previous works.

Keywords: Carbopol®, Rayleigh-Bénard convection, yielding
, rheological hysteresis, supercritical bifurcation

Email address: Teodor.Burghelea@univ-nantes.fr (Teodor Burghelea)

Contents

List of Figures

1. Introduction

The Rayleigh-Bénard convection in a fluid heated from below is a paradigm of pattern forming systems, Cross and Hohenberg (1993).

Imposing a vertical temperature gradient within a Newtonian fluid by heating it from below translates into a vertical gradient of the fluid density or buoyancy which, beyond a critical value of the temperature gradient ΔT_c, may overcome the viscous dissipation and and trigger an upwards motion of the fluid elements. Within a finite size system and in the virtue of the mass conservation, this instability results into a regular and periodic fluid motion in the form of rolls which is classically referred to as the Rayleigh-Bénard thermal convection.

The transition to laminar Rayleigh-Bénard convection in Newtonian fluids has been intensively studied during the past five decades both theoretically and experimentally. Among a large amount of published work on the topic, we can refer the reader to textbook of Koschmeider Koschmieder (1993) and the review article by Bodenschatz, Pesch and Ahlers , Bodenschatz et al. (2000).

A Newtonian fluid heated from below loses its hydrodynamic stability when the stresses associated to the buoyancy forces exceed those associated to the viscous dissipative forces.

The balance between the buoyancy and the viscous forces is quantified by the Rayleigh number:

$$Ra = \frac{\beta \Delta T g H^3}{k \cdot \nu} \tag{1}$$

where β is the coefficient of thermal expansion, g the gravitational constant, k the thermal diffusivity, ν the kinematic viscosity, ΔT the temperature difference measured between the plates and H is the distance between plates. It has been shown both theoretically and experimentally that the onset of the convection corresponds to $Ra_c \approx 1708$.

Whereas there exists an overwhelming number of fundamentally important studies of the Rayleigh-Bénard convection in Newtonian fluids, much less progress has been achieved in understanding the thermal convection in non-Newtonian fluids. The reason for this most probably originates in the highly non trivial coupling between the hydrodynamic problem, the rheological properties of the fluids and their thermal dependence.

There exist several systematic studies of the Rayleigh-Bénard convection in viscoelastic fluids focusing on the role of elasticity (quantified by the Weissenberg number) on the onset of convection and on the main features of the transition, Park and Ryu (2001); Park and Park (2004); Lamsaadi et al. (2005).

Yield stress fluids represent a broad class of materials made of high molecular weight molecular constituents which, loosely speaking, display a solid-like behaviour as long as the stress applied onto them does not exceed a critical value called the yield stress, τ_y, and a fluid one beyond this threshold.

The constantly increasing level of interest of both theoreticians and experimentalists in yield stress materials has, in our opinion, a two-fold motivation. From a practical perspective, such materials have found an increasing number of practical applications for several major industries (which include foods, cosmetics, pharmaceutical oil field, etc.) and they are encountered in the daily life in various forms such as food pastes, hair gels, emulsions, cement, mud and more. Such materials are also relevant to various geophysical flows such as magma flows within the Earth's mantle, Griggs (1939); Meinesz (1947); Orowan (1965); Le Bars and Davaille (2004).

Systematic studies of the hydrodynamic stability of yield stress fluids have been performed only recently, Frigaard et al. (1994); Landry et al. (2006); Metivier et al. (2005). In this context, there exist several fundamental mathematical and physical problems yet to be understood. One of these problems concerns with the occurrence of the Rayleigh-Bénard instability in yield stress materials.

The very first theoretical study of the Rayleigh-Bénard convection in a yield stress fluid was performed by Zhang and her coworkers, Zhang et al. (2006). Using a linear stability approach formulated within the framework of the Bingham rheological model, they show that base state is stable to infinitesimally small perturbations regardless the finite value of the yield stress. This is due to the fact that, corresponding to the stable base flow state, the Bingham model predicts an infinite viscosity which can not be destabilised by infinitesimally small perturbations.

The weakly nonlinear stability analysis performed by Balmforth and Rust Balmforth and Rust (2009) carried out within the framework of the Bingham rheological model indicates that a sufficiently large finite amplitude perturbation of the base state of a viscoplastic fluid may trigger Rayleigh-Bénard convection. Their theoretical analysis is complemented by preliminary experiments by which they have convincingly visualised by means of a coloured dye the convective rolls in a layer of Carbopol® heated from below.

A numerical simulation study of the Rayleigh-Bé convection of a Bingham fluid in a square enclosure is presented by Turan et al., Turan et al. (2012). By a systematic scaling analysis Turan and his coworkers assess the scaling of the relevant non-dimensional numbers corresponding to the onset of the instability and discuss them and relate them to the strength of the gel.

An experimental study of the development of thermal plumes within a Carbopol® gel due to local heating was recently presented by Davaille and her coworkers, Davaille et al. (2013). Depending on the ratio between the thermally induced stresses and the yield stress quantified by the yield number Y, they have observed three distinct dynamic regimes: stable, small scale convective (the convection is localised around the heater) and thermal plumes. A systematic description of the morphology of the thermal plumes is provided as a function of the yield number. The study by Davaille et al. reinforces the main conclusion of the study by Balmorth and Rust that finite amplitude perturbations may indeed destabilise the base flow of fluids with a finite yield stress.

Darbouli and his coworkers have studied experimentally the Rayleigh-Bénard convection within various Carbopol® gels confined in a cylindrical cavity and heated from below, Darbouli et al. (2013). Although they did not intentionally

applied a finite amplitude perturbation, they did observe convective states various values of the yield stress that cover a limited range, [0.0047 Pa - 0.104 Pa] (according to their Table 1).

In the case of a viscoplastic fluid, the onset of the Rayleigh-Bénard convection coincides with the onset of the solid-fluid transition (yielding) and thus, the viscous stresses are infinite at the onset. This suggests that, in the case of a viscoplastic fluid, the onset condition should be reconsidered. For this purpose, the force balance criterion can be modified by considering that the thermal convection is triggered when the stresses associated to the buoyancy overcome the yield stress τ_y of the gel and by replacing the viscous time scale with a characteristic time scale associated to the microstructure of the gel:

$$Ra = \frac{\rho\beta\Delta T g H}{\tau_y}\frac{t_d}{t_g} \geq Ra_c \tag{2}$$

Here $t_d = \frac{H^2}{\kappa}$ is the characteristic time scale associated to the thermal diffusion and t_g is a characteristic time scale associated to the gel microstructure near the onset of the convection (i.e. near the yield point) which will be discussed in detail through our paper in connection to the rheological properties of the Carbopol® gels.

From a phenomenological point of view and following the basic ideas of the (energy) *balance theorem* initially introduced by Chandrasekhar (see Ref. Chandrasekhar (1961)) one can alternatively consider that the thermal convection in a yield stress fluid is initiated when the energy dissipated per unit volume of material by the buoyancy forces becomes comparable in magnitude to the maximal elastic energy that the gel network can locally store per unit volume prior to yielding: $W_b \geq W_e$. Here $W_e = \rho g\beta\Delta T$ is the energy dissipated per unit volume by the buoyancy forces and $W_e = \tau_y$ is the elastic energy per unit volume. With these considerations, the energy criterion for the convective instability in a yield stress fluid can be formulated in terms of the yield number Y:

$$Y = \frac{\tau_y}{\rho\beta g H\Delta T} \leq Y_c \tag{3}$$

To our best knowledge, there exists no experimental assessment of the validity of the force and energy balance criteria for the transition to thermal convective states in a Carbopol® gel given by Eqs. 2 and 3.

The present study concerns with an experimental investigation of the Rayleigh-Bénard convection in Carbopol® gels with various concentrations (yield stresses). Among the primary goals of the study we mention the accurate detection of the onset of the instability in relation with the rheological properties of the gel (yield stress), the characterisation of the convective flow patterns as a function of the control parameter. Of particular interest is the assessment of the nature of the bifurcation towards convective states which is little documented by the existing body of experimental work. In addition to these goals, we are interested in the scaling of the physical parameters characterising the onset of the convective instability with the rheological properties of the solutions which will allow one to probe the applicability of the force and energy balance stability criteria discussed above.

The paper is organised as follows. The experimental setup and the measuring techniques are presented in Sec. 2. The choice, preparation and the thermal and rheological characterisation of the working fluids are discussed in Sec. 2.1. The Rayleigh-Bénard experimental setup and the measuring techniques are described in Sec. 2.2. Within this section, a concise assessment of the reliability of the measuring techniques is made. The experimental results are presented in Sec. 3. To probe the reliability of both the experimental setup and the measuring techniques, a systematic experiments performed with a Newtonian solution with known physical properties are presented in Sec. 3.1 and the results are compared with both previous results and theoretical predictions.

The experimental results concerning yield stress fluids with various yield stresses are presented in Sec. 3.2. Sec. 3.3 is devoted to a comparison of our experimental findings with both existing theoretical predictions and previous experimental results. The paper closes with a summary of our main findings and a brief discussion their possible impact on the current understanding of the emergence and basic physical features of the Rayleigh-Bénard convection in viscoplastic fluids, Sec. 4.

2. Experimental setup and methods

2.1. Choice, preparation, thermal and rheological characterisation of the viscoplastic fluids

Carbopol® resins are synthetic polymers of acrylic acid initially introduced over six decades ago (B.F. Goodrich Co.). They are cross-linked with various chemical compounds such as divinyl -glycol, allyl-sucrose, polyalkenyl

polyether etc. In an anhydrous form, the average size of the polymer molecules is of the order of hundreds of nanometers. In the absence of crosslinks, the polymer particle can be viewed as a collection of linear chains intertwined (in a coiled state) but not chemically bonded. The Carbopol® microgel particles are soluble in polar solvents and, upon dissolution, each individual polymer molecule hydrates, partially uncoils, and swells several orders of magnitude. Addition of a neutralising agent leads to the creation of negative charges along the polymer backbone due to ionisation of the carboxylic acid groups. Consequently, swollen polymer molecules crosslink, forming a system of microgel particles. The microgel system can sustain finite deformations (behaving like an elastic solid) prior to damage. When local applied stresses exceed a threshold value the gel system breaks apart and the material starts to flow. This is the commonly accepted microscopic scale origin of the macroscopic yielding of the material.

Various solutions of Carbopol® 980 with concentrations ranging in between 0.05% and 0.11% (by weight) have been used as a working fluids. The procedure for the preparation of the solution is described as follows. First, the right amount of anhydrous Carbopol® 980 has been gently dissolved in water while continuing stirring the mixture with a commercial magnetic stirring device. The stirring process was carried on until the entire amount of polymer was homogeneously dissolved. A particular attention has been paid to the homogeneity of the final mixture, which has been assessed visually by monitoring refractive index contrast. Next, the pH of the mixtures (initially around 3.2, due to the dissociation of the polyacrylic acid in water) has been brought to a neutral value by addition of about 140 parts per million (ppm) of sodium hydroxide ($NaOH$). The final value of the pH has been carefully monitored using a digital pH- meter (from Grosseron). Upon the ionisation and the neutralisation of the carboxylic groups of the polyacrylic acid, the Carbopol particles swell dramatically forming a percolated micro-gel, Piau (2007). As a particular attention has been paid to control the neutral pH, the concentration of the sodium ions was presumably equal to that of the carboxylate groups. To homogenise the gelled mixture, the fluid has been stirred with a propeller mixer (at 400 rpm) for about two hours and then allowed to rest for several more hours. Prior to each rheological test, the air bubbles entrapped into the gel during the stirring process have been removed by placing the samples in a low pressure chamber for 30 minutes. Finally, the fluid batch has been stored at room temperature in a sealed container in order to minimise the evaporation of the solvent.

The rheological properties of the solutions were investigated using a Mars III (from Thermofischer) equipped with a Peltier system able to control the temperature with an accuracy better than $0.1^{\circ}C$ and a nano-torque module which allows one to accurately explore very small rates of deformation, $\dot{\gamma} \approx 10^{-5}\ s^{-1}$. The radius of the parallel plates is $R = 40\ mm$ and the gap measured by the rheometer is $d = 1\ mm$. To prevent the wall slip which is known to be a major concern during the rheological investigation of Carbopol gels the parallel plates have been sandblasted. We have checked that no significant slip occurred by performing subsequent measurements on the same gel sample with various gaps and assessing their reproducibility.

The stress per each step of the linear shearing ramp was maintained constant for a time $t_0 = 2\ s$. The choice of this protocol as opposed to the classical steady state flow ramps ($t_0 \to \infty$) typically employed in the characterisation of the yield stress materials may seem controversial to some and deserves a separate argumentation.

The choice of a stepped stress ramp over the classical steady state rheological protocols was motivated by the fact that the flow kinematics in the Rayleigh - Bénard configuration is not compatible with a steady state. This is because above the onset of the convection, the local stress applied onto individual fluid elements changes in a continuous manner as the elements move along the Lagrangian trajectories.

Performing increasing/decreasing controlled stress ramps has also an important practical advantage. It has been previously pointed out by several authors that the classical method of determining the yield stress by fitting the flow curves by the Herschel-Bulkley model is typically prone to errors which, depending on the value of the yield stress, may be as large as 20% of the measured value Kim et al. (2003); Uhlherr et al. (2005); Piau (2007).

Among the reasons for this significant errors we point out the uncertainty in determining the fully yielded part of the flow curve where the Herschel-Bulkley model is expected to work [1]. In addition to this argument, performing increasing/decreasing controlled stress ramps also provides an accurate method of determining the fully yielded part of the flow curve by monitoring the range where the deformation states are fully reversible (the two branches of the flow curve overlap).

[1] Note that, due to the strongly non-linear nature of the Herschel-Bulkley model, the outcome of classical non-linear regression algorithms such as the Levenberg-Marquardt algorithm is very sensitive to the number of the data points considered and their range.

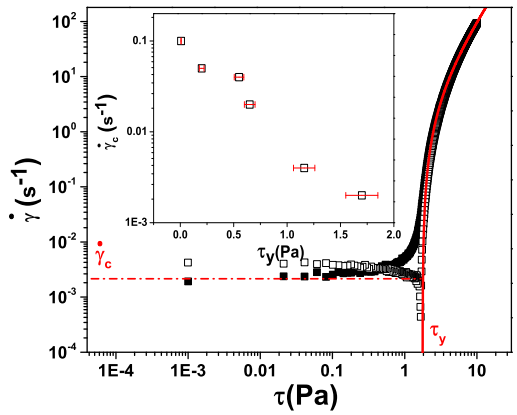

Figure 1: Dependence of the absolute value of the shear rate $|\dot{\gamma}|$ on the applied stress τ for a Carbopol® solution with the concentration $c = 0.115\%$. The full/empty symbols refer to the increasing/decreasing branch of the stress ramp, respectively. The data were acquired at room temperature, $T = 294.3K$. The full line is a non linear fitting function according to the Herschel-Bulkley model with $\tau_y = 1.76 \pm 0.005Pa$, $K = 0.727 \pm 0.003\ Pas^{-n}$, $n = 0.53 \pm 9.15 \cdot 10^{-4}$. $\dot{\gamma}_c$ stands for the critical rate of shear corresponding to the end of the elastic solid deformation regime. The dependence of the critical rate of shear $\dot{\gamma}_c$ on the yield stress τ_y is presented in the insert.

A typical experimental result obtained following the protocol described above and using serrated parallel plates is illustrated in Fig. 1.

As the applied stress is gradually increased, three deformation regimes are observed. For low stress values an elastic solid deformation regime consistent with Hooke's law is observed [2]. For the largest values of the applied stress investigated a fluid (fully yielded) regime is observed. This deformation regime is well described by the Hershel-Bulkley model, $\tau = \tau_y + K|\dot{\gamma}|^n$, Herschel and Bulkley (1926). Here τ_y, K and n stand for the yield stress, consistency and power law index, respectively. The transition between the solid and the fluid regime is not direct but mediated by an intermediate regime where solid and fluid bands coexist, Fig. 1. It is equally important to note that, unlike previously considered, the deformation regimes are reversible upon increasing/decreasing external forces *only* within the fully yielded regime.

The dependence of the critical rate of deformation $\dot{\gamma}_c$ corresponding to the elastic solid regime on the yield stress τ_y is presented in the insert of the Fig. 1. The measurements of the critical rate of shear associated to the solid-fluid transition allows one to estimate the characteristic time of the material t_g involved in the definition of the plastic Rayleigh number given by Eq. 2 as $t_g \approx \dot{\gamma}_c^{-1}$.

A more detailed and systematic discussion together with a simple model able to capture these previously unnoticed features are presented in Ref. Putz and Burghelea (2009) which, to our best knowledge, is the first experimental work that has demonstrated that in spite of the nearly universal picture of Carbopol® gels as non-thixotropic model yield stress fluids, time dependent effects do play a crucial role during their yielding process.

Measurements of the yield stress τ_y within the entire range of Carbopol® concentrations explored through the Rayleigh-Bénard convection experiments are presented in Fig. 2. The error bars are defined by the fitting error of the Levenberg-Marquardt algorithm with the Herschel-Bulkley model. Quite interestingly, although we have worked within similar ranges of Carbopol® concentrations as Darbouli and his coworkers, we have been unable to reproduce their surprisingly small values of yield stress, Darbouli et al. (2013). Below a critical value of the Carbopol® concentration c^* usually referred to as the overlap concentration, the solutions exhibit no measurable yield stress but only a weakly shear thinning behaviour. Beyond the overlap concentration c^* the measured yield stress τ_y scales linearly with the polymer concentration. A phenomenological discussion of the physicochemical properties of the Carbopol® mi-

[2] Bearing in mind that the stress ramp is linear in time, $\dot{\gamma} \approx constant$ translates into a proportionality relation between the applied stress τ and the strain γ.

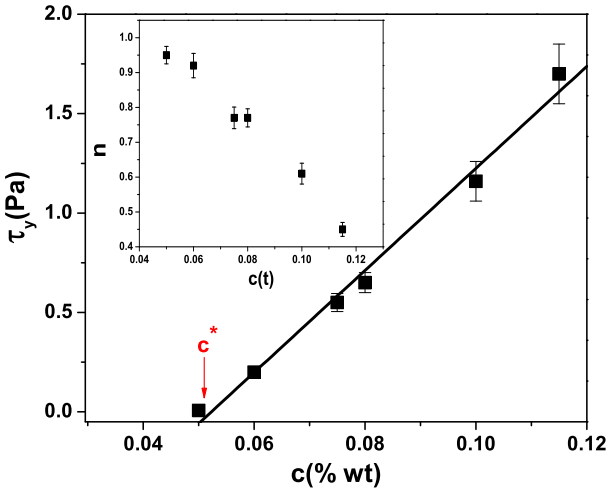

Figure 2: Dependence of the yield stress τ_y on the Carbopol® concentration. The error bars are defined by the fitting error of the Levenberg-Marquardt algorithm with the Herschel-Bulkley model. The full line is linear fit. Here c^* stands for the overlap concentration. The dependence of the power law index n on the Carbopol® concentration is presented in the insert.

$\mathbf{c}(\%\mathbf{wt})$	$\beta(\mathbf{10^{-4}K^{-1}})$	$\mathbf{c_p}(\mathbf{Jkg^{-1}K^{-1}})$	$\kappa(\mathbf{10^{-7}m^2\,s^{-1}})$	$\alpha(\mathbf{W/mK})$	$\rho(\mathbf{kg\,m^{-3}})$	$\tau_\mathbf{y}(\mathbf{Pa})$
0.05	2	4231.63	1.5	0.61	961 ± 96	$0.007 \pm 7 \cdot 10^{-4}$
0.06	2	4245.77	1.48	0.61	970 ± 97	0.2 ± 0.022
0.075	2	4202.79	1.44	0.6	990 ± 105	0.55 ± 0.045
0.08	2	4176.13	1.45	0.6	990 ± 99	0.65 ± 0.05
0.1	2	4119.47	1.44	0.6	1010 ± 101	1.16 ± 0.1
0.115	2	3998.44	1.48	0.61	1030 ± 103	1.7 ± 0.15

Table 1: Physical and rheological properties of the Carbopol® solutions used in our study: β - thermal expansition coefficient, c_p - heat capacity, κ - thermal diffusivity, α - thermal conductivity, ρ - density, τ_y - yield stress. The densities were measured at room temperature, $T = 23\,^oC$.

crostructure is presented in Ref. Weber et al. (2012). This experimentally found dependence of the yield stress on the polymer concentration is (for this grade of Carbopol®) at odds with the semi-empirical derivation presented in Ref. Piau (2007) which leads to a cubic dependence but agrees very well with the measurements presented in Ref. Bertola (2009) (see Fig. 1 therein). Within the range of polymer concentrations explored through our convection experiments, a clear shear thinning behaviour manifested through values of the power law index n smaller than unity is observed, see the insert in Fig. 2. The yield stress measurements presented in Fig. 2 demonstrate that, within the range of polymer concentrations explored through the Rayleigh-Bénard convection experiments, the working solutions exhibit both a yield stress and a shear thinning behaviour.

The density of the solutions has been measured by carefully weighting (with an accuracy of 1 mg) fixed volumes of solutions.

The thermal properties of the Carbopol® gels have been investigated using a hot disk thermal conductivity analyser ($C-Therm$, model TC_5). The measured values of the thermal conductivity α of the heat capacity c_p and of the thermal diffusivity κ are listed in Tab. 1. We note that each of these thermal properties are, within the instrumental accuracy, practically independent on the Carbopol® concentration.

2.2. Experimental apparatus and measuring techniques

The experimental setup is schematically illustrated in Fig. 3. It consists of a rectangular cavity with acrylic made flat transparent walls. The length of the fluid cavity is $L = 386\ mm$, the width $W = 186\ mm$ and its height is

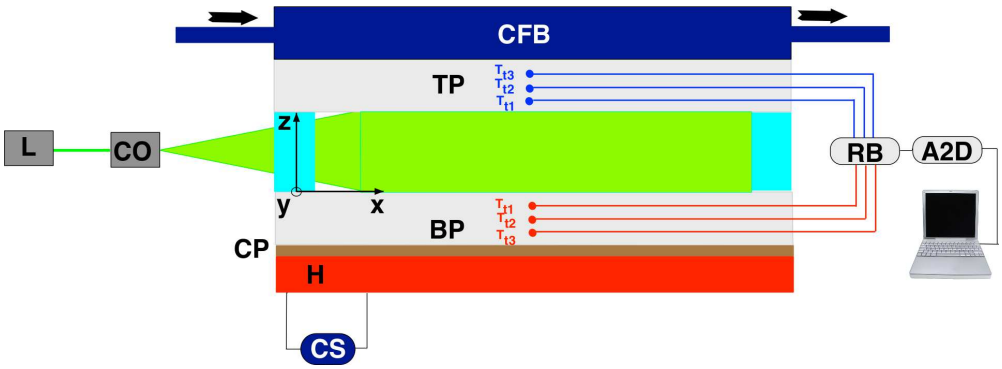

Figure 3: Schematic view of the experimental setup **L** - solid state laser, **CO** - cylindrical optics block, **CP** - copper plate, **TP** - top plate, **BP** - bottom plate, **CFB** - cooling fluid bath, **A$_2$D** - analogical to digital signal conditioning block, **RB** - reference box.

$H = 20\ mm$. The bottom and the top enclosures of the cavity are 3 cm thick polycarbonate plates. The significant width of these two plates and their small thermal conductivity coefficient have been purposely chosen in order to obtain a uniform temperature distribution along the entire fluid cavity.

By means of infrared imaging of the convection cell, it has been checked that the temperature uniformity along the convection cell is better than 5%, Fig. 5.

The bottom plate was heated electrically by a resistive circuit fed by a constant current I supplied by the stabilised current supply **CS**. The heating power was calculated as $P = RI^2$ where $R = 25.5\ \Omega$ is the resistance of the electrical heater. To avoid the thermal damage of the bottom polycarbonate plate, a copper plate **CP** is interposed in between the polycarbonate plate and the resistive heater.

The top plate was uniformly cooled by means of a circulating fluid bath **CFB**. The circulating fluid is a mixture of glycerin and anti-freeze and its temperature is maintained constant through our experiments, $T_{wb} = -10^oC$.

The transition to the Rayleigh-Bénard convection was simultaneously investigated by both integral measurements of the temperature difference ΔT between plates and local measurements of the amplitude of the convective states.

A major challenge during the integral measurements was to accurately measure the temperature difference between the plates as a function of the heating power P without perturbing the fluid (which is crucial while assessing its hydrodynamic stability), i.e. in a non invasive way. For this purpose, three thermocouples (type K) have been embedded in each polycarbonate plate at precise vertical positions z, Fig. 4(a). The signals of the thermocouples are passed to the digitising block **A$_2$D** via the reference box **RB**. The linear dependence of the indications of each triplet of thermocouples on their vertical position z [3] is extrapolated at the contact points between the plates and the working fluid (the full symbols in Fig. 4(a)) and the difference $\Delta T = T_b - T_t$ is recorded.

An additional concern during the integral measurements of the temperature difference ΔT during the convection experiments was related to avoiding the transient regimes. For this purpose, prior to each reading, the time series of the temperature difference ΔT were recorder for extended time periods (up to 18 hours), Fig. 4(b). Before reaching a steady state, two transient parts can be observed in the time series of the temperature difference ΔT. The first transient observed prior to reaching a maximal temperature difference ΔT_{max} is of conductive nature and can be fitted by (see the full line in Fig. 4(b)):

$$\Delta T = \Delta T_{max}\left[1 - e^{\frac{t_0 - t}{t_d}}\right] \tag{4}$$

Here t_d is the thermal diffusion time defined in Sec. 1. If one uses the thermal expansion coefficient listed in Tab. 1 for the Carbopol® solutions used in our experiments the thermal diffusion time can be estimated as $t_d \approx 2730\ s$.

The dependencies of the characteristic diffusion time t_d on the heating power P for both increasing (full symbols) and decreasing (empty symbols) values of the heating power and measured for three distinct Carbopol® solutions are

[3] Note that within the polycarbonate plates there exists only a conductive heat transfer.

presented in the insert of Fig. 4(b). The error bars are defined by the error of the nonlinear fit of the first transient part of the time series of the temperature difference between the plates ΔT by Eq. 4. As expected and for each value of the polymer concentration the characteristic diffusion time is independent on both the heating power P and the polymer concentration. The invariance of t_d with the polymer concentration is consistent with the independence of the thermal conductivity of the solutions on the polymer concentration, see Tab. 1. The measured values of the characteristic diffusion time are comparable to the theoretical estimate, though slightly larger.

The second transient observed after the maximum of the time series of the temperature difference is of convective nature and can be described within the framework of the Landau theory (see, for example the book by Chandrasekar for details, Chandrasekhar (1961)) by (the dash-dotted line in Fig. 4(b)):

$$\Delta T = \Delta T_\infty + De^{\frac{-2t}{t_c}} \tag{5}$$

where $\Delta T_\infty = lim_{t-\infty}\Delta T(t)$ is the steady state value of the temperature difference.

The characteristic time t_c is the characteristic time that governs the formation of the convection rolls and reflects the nonlinear dynamics of the system near the onset of the convective instability in the framework of the Landau theory.

For each value of the heating power P, the temperature difference ΔT was recorded **only** after sufficiently long time periods $t > t_d + t_c$ when all the transients have disappeared and the signal reached a steady state. We emphasise that ignoring the duration of these transients during convection experiments can result in seriously flawed conclusions on the nature of the bifurcation towards convective states and this issue deserves the uttermost care of the experimentalists.

Together with the integral measurements of the dependence of the temperature difference between plates ΔT on the heating power P, the transition to the Rayleigh-Bénard convection has been investigated by local measurements of the convective pattern amplitude by the Digital Partical Image Velocimetry (**DPIV**) technique.

For this purpose, a green laser beam ($\lambda = 514\ nm$) with a power of 500 mW emitted by the solid state laser **L** (from Changchun Industries, Model LD-WL206) is deflected by a mirror through a cylindrical optics block **CO** which reshapes it in a horizontal laser sheet, Fig. 3. The cylindrical optics block is composed of a glass rod with a short focal distance $f_1 \approx 2\ mm$ and a cylindrical lens with a larger focal distance, $f_2 \approx 5\ cm$. The two optical elements are mounted orthogonally to each other and in a telescopic arrangement such as the primary horizontal laser sheet generated by the glass rod is focused on the vertical direction in the middle of the flow channel by the second lens minimising thus its thickness in the measurement region. The thickness of the generated laser sheet is roughly $80\mu m$ in the beam waist region which is positioned at the centreline of the convection cell. The working fluid was seeded with an amount of 200 parts per million (ppm) of polyamide particles with a diameter of 60 μm (from Dantec Dynamics).

Time series of the velocity fields were obtained by a iterative multi-grid **DPIV** algorithm implemented in the house under Matlab®, Scarano and Rhiethmuller (2001); Raffel et al. (September 2007).

For this purpose, a sequence of flow images has been acquired at a frequency of 2 frames per minute during three minutes. Right above the onset of the thermal convection, several flow images have been skipped in order to increase the inter-frame and maintain the average displacement of the tracer particles in the optimal range of 5 to 15 pixels. We note that the maximal number of frames that may be skipped without a critical smearing out of the peaks of the 2-dimensional correlation of the interrogation windows is limited by both the stability of the laser source and the characteristic flickering time of the brightness of individual scattering flow tracers which is mainly related to the size of the tracer particle and viscosity of the solution. Thus, by skipping up to 40 frames, we have artificially increased the inter-frame between the images passed to the **DPIV** algorithm up to 20 minutes which allowed one to measure flow speeds as small as a $1\mu m/s$ around the onset of the instability.

Together with this, the size of the smallest interrogation window has been adapted to the mean flow velocity corresponding to value of the heating power (i. e. distance from the onset of the convection). The spatial resolution of the measured flow fields was 400 μm. Using this adaptive **DPIV** protocol the instrumental error of the measured velocity fields does not exceed 7% through all our experiments (the upper error bound given here corresponds to measurements near the onset of the convection).

A practical limitation of the **DPIV** technique described above is related to the sedimentation of the seeding particles during the long waiting times needed to reach a state of thermal equilibrium (which can reach up to 12 hours,

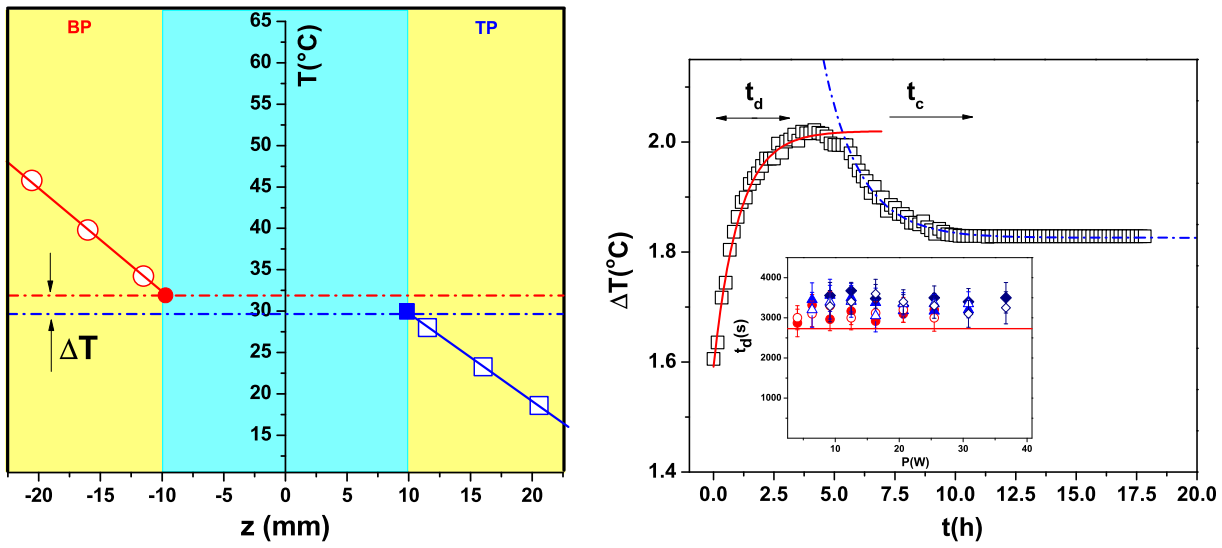

Figure 4: (a) Temperature measurements within the bottom plate **BP** (the empty circles) and within the top plate **TP** (the empty squares). The full lines are linear fitting functions and the full symbols are the linear extrapolations of the temperature measurement at the contact points with the fluid. (b) Time series of the temperature difference ΔT. The full line is a nonlinear fit by Eq. 4. τ_d stands for the characteristic thermal diffusion time. The dash-dotted line is a fit according to Eq. 5. τ_c stands for the characteristic slowing down time. The dependence of the thermal diffusion time t_d on the heating power P measured for three Carbopol® solutions with the concentrations $c = 0.06\%, 0.075\%, 0.08\%$ for both increasing (full symbols) and decreasing (empty symbols) heating powers is presented in the inset. The full line is the theoretical estimate, $t_d \approx 2730\ s$ (see text).

see Fig. 4(b) and the corresponding discussion). Thus, for the two lowest Carbopol® concentrations we have investigated, a full characterisation of the flow fields over the entire range of heating powers was not possible due to the sedimentation of the seeding particles during the long waiting times.

An important concern related to the reliability of our measurements was related to the uniformity of the temperature distribution along the convection cell (the x direction).

To quantitatively assess the uniformity of the temperature distribution along the convection cell, the system has been imaged frontally with a infra-red camera (Fluke, model *Ti* 20), Fig. 5. We have found that, along the horizontal axis x the temperature varied less than 3% of its mean value at the mid-point between the parallel plates, $z = H/2$.

To avoid boundary effects which may significantly alter the nature of the bifurcation towards convective states, Brown and Setwartson (1978); Brown and Stewartson (1979), the local **DPIV** measurements of the convective amplitudes have been conducted at $x \approx L/2$ (within the region highlighted by a rectangle in Fig. 5) and $y \approx W/2$.

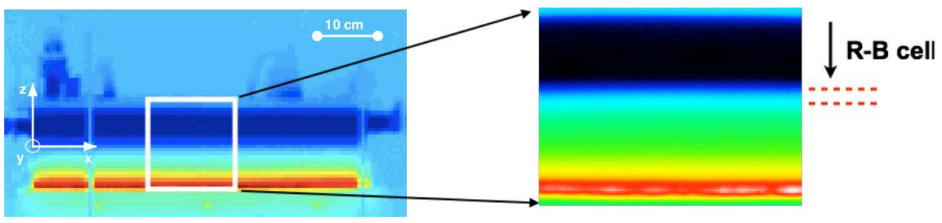

Figure 5: Infrared image of the convection cell. The magnified insert presented on the right side provides a zoom-in into the gap between the the top and the bottom plates of the cell. The colour is coded from blue (cold) to red (hot).

3. Experimental results

3.1. Validation of the experimental setup and measuring techniques with a Newtonian fluid

Prior to characterising the transition to the Rayleigh-Bénard convection within a Carbopol® gel, we have focused on a systematic validation of the experimental system and the measuring techniques with a Newtonian fluid, pure Glycerin. The experimentally measured values of the physical parameters for the Glycerin are: $\beta = 5 \cdot 10^{-4} K^{-1}$, $g = 9.8 m^2/s$, $\kappa = 1.37 \cdot 10^{-7} m^2/s$ and $\nu = 872 \cdot 10^{-6} m^2 s^{-1}$.

Measurements of the temperature difference ΔT between the plates performed with a Glycerin solution for both increasing and decreasing values of the heating power P are presented in Fig. 6, A linear increase of the integral temperature difference between the plates ΔT with P which corresponds to a purely conductive heat transfer regime (the slope of this dependence is proportional to the thermal conductivity of fluid) is observed below a critical value of the heating power $P_c \approx 16.32W$. Beyond this onset the dependence becomes sub nonlinear consistently with a mixed conductive-convective heat transfer regime. Based on the material parameters enumerated above, the critical Rayleigh number corresponding to the onset of the thermal convection can be estimated $Ra_c \approx 1774$ which is in a fair agreement with the theoretical value $Ra_c^t = 1708$ given in Chandrasekhar (1961).

The dependence of the reduced temperature difference $\Delta T_r = \frac{\Delta T}{\Delta T_{lin}} - 1$ on to the reduced power $P_r = P/P_c - 1$ is presented in Fig. 7 (a). Here ΔT_{lin} represents the linear temperature difference measured within the conductive regime (see the full line in Fig. 6). In agreement with the theoretical predictions for the convective instability in Newtonian fluids, the reduced temperature difference ΔT_r increases linearly with the reduced heating power.

Measurements of the convection amplitude obtained via the **DPIV** technique described in Sec. 2.2 as a function of the heating power are presented in Fig. 7. Above the onset of convection the velocity amplitude follows a square root dependence on the heating power, $V = A\sqrt{\frac{P}{P_c} - 1}$, according to the Landau theory of imperfect bifurcations. This result agrees with both theoretical predictions Newell and Whitehead (1969); Segel (1969) and previous experimental findings, Dubois and Bergé (1978).

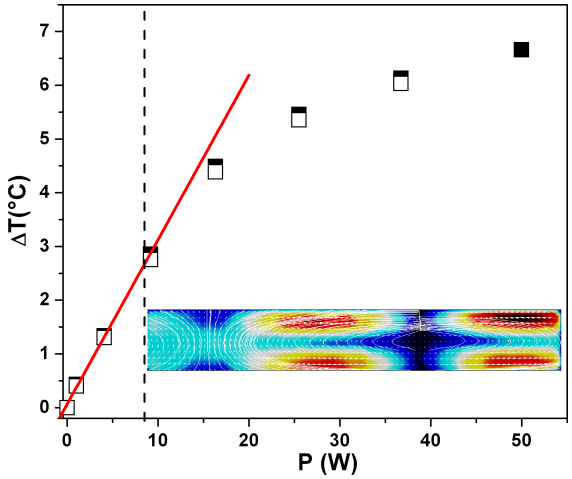

Figure 6: Dependence of the temperature gradient ΔT within Glycerin on the heat flux P. The full/empty symbols refer to increasing/decreasing heat flux. The vertical dashed line marks the transition between the conductive and convective regimes. A typical **DPIV** measured convection pattern is illustrated in the insert.

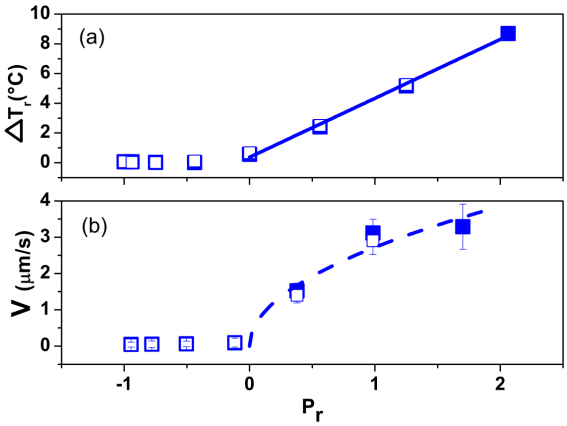

Figure 7: **(a)** Dependence of the reduced temperature ΔT_r on the reduced power. The line is a linear fit. **(b)** Dependence of the pattern amplitude V on the reduced power P_r. The line is a Landau fit.

To conclude this part, the measurements illustrated and discussed above clearly identify the transition to convective states within a Newtonian fluid as an imperfect bifurcation in agreement with both theoretical predictions and previous experimental results.

After having probed by these measurements the reliability of our experimental setup and measuring methods, we focus in the following section on the transition to the Rayleigh-Bénard convection in various Carbopol® gels.

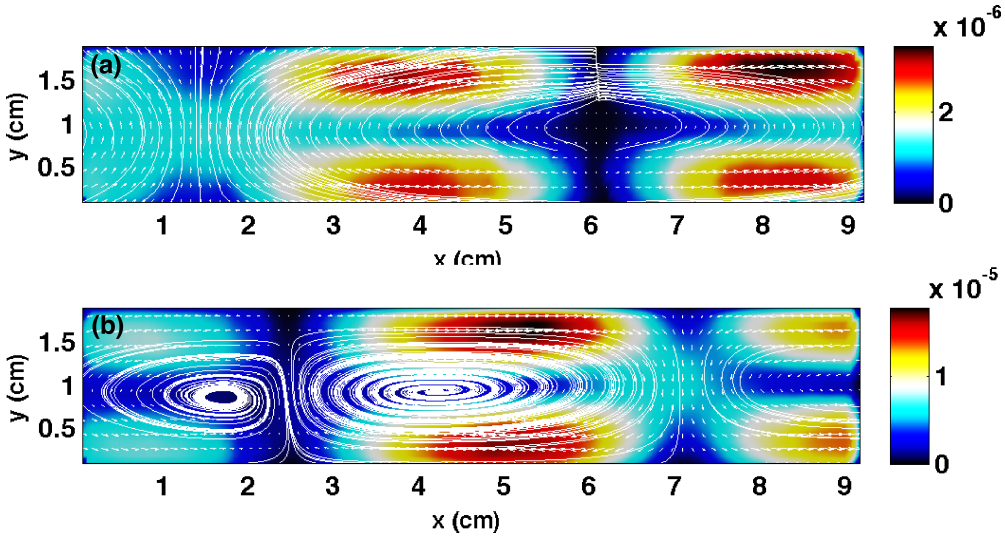

Figure 8: Measured flow patterns for: **(a)** Glycerin solution **(b)** Carbopol® solution with $c = 0.075\%$. The false colour map refers to the absolute value of the flow speed and the full lines are stream lines. For a better clarity, the velocity field has been down-sampled by a factor of 2 along each axis.

3.2. Observation and characterisation of the Rayleigh-Bénard convection in various Carbopol gels

After the systematic validation of the experimental system and of the measuring techniques presented in Sec. 3.1 we now turn our attention to the experimental observation of the Rayleigh-Bénard convection for various Carbopol® solutions with weight concentrations ranging in between 0.05% and 0.11%.

As already discussed in Sec. 2.1 and illustrated in Fig. 2, the chosen polymer concentrations lie all above the overlap concentration c^* which insures that our working fluids are indeed yield stress fluids not just weakly shear thinning.

The transition to convective states within various Carbopol® gels is simultaneously assessed by both local flow speed measurements by the **DPIV** technique and integral measurements of the temperature difference between the top and the bottom plates, ΔT.

For each value of the concentration of the Carbopol® solution, no measurable flow is observed if the integral temperature difference between plates does not exceed a critical value, $\Delta T < \Delta T_c$. As the temperature difference is increased past this onset, the energy dissipated per unit volume of material by the buoyancy forces overcomes the elastic energy associated the gel microstructure. Consequently, the gel locally yields and roll flow patterns are observed. The unstable flow patterns are observed in the absence of an external perturbation of a finite amplitude.

The comparison of the viscoplastic convective flow patterns with their Newtonian counterpart observed with a Glycerin solution is presented in Fig. 8.

For the case a Carbopol® solution an interesting feature of the flow field can be observed in the vicinity of the top/bottom plates of the convection cell: the convection rolls are practically flat near the solid boundaries and the stream lines display a zero curvature almost along the entire extent of the convection roll. This difference with respect to the Newtonian counterpart may be related to significant topological and structural differences in the velocity boundary layers (also note that the Carbopol® gels slip at the level of the smooth solid boundaries).

The evolution of the flow patterns as the control parameter is varied right above the onset of the convection monitored within a 0.08% Carbopol® solution is illustrated in Fig. 9.

Right above the onset of the convection ($\Delta T = 3.18^oC$), the flow pattern has a slightly asymmetric appearance. This may be due to the large characteristic times t_c needed for the pattern to reach a steady state or the so called *critical slowing down* phenomenon which will be discussed in detail trough paper. Upon an increase of the temperature difference between plates the flow patterns become more regular and the horizontal extent λ of the convection rolls decreases (equivalently with an increase of the horizontal wave number $q_x = \frac{2\pi}{\lambda}$). It is important to note that the flow

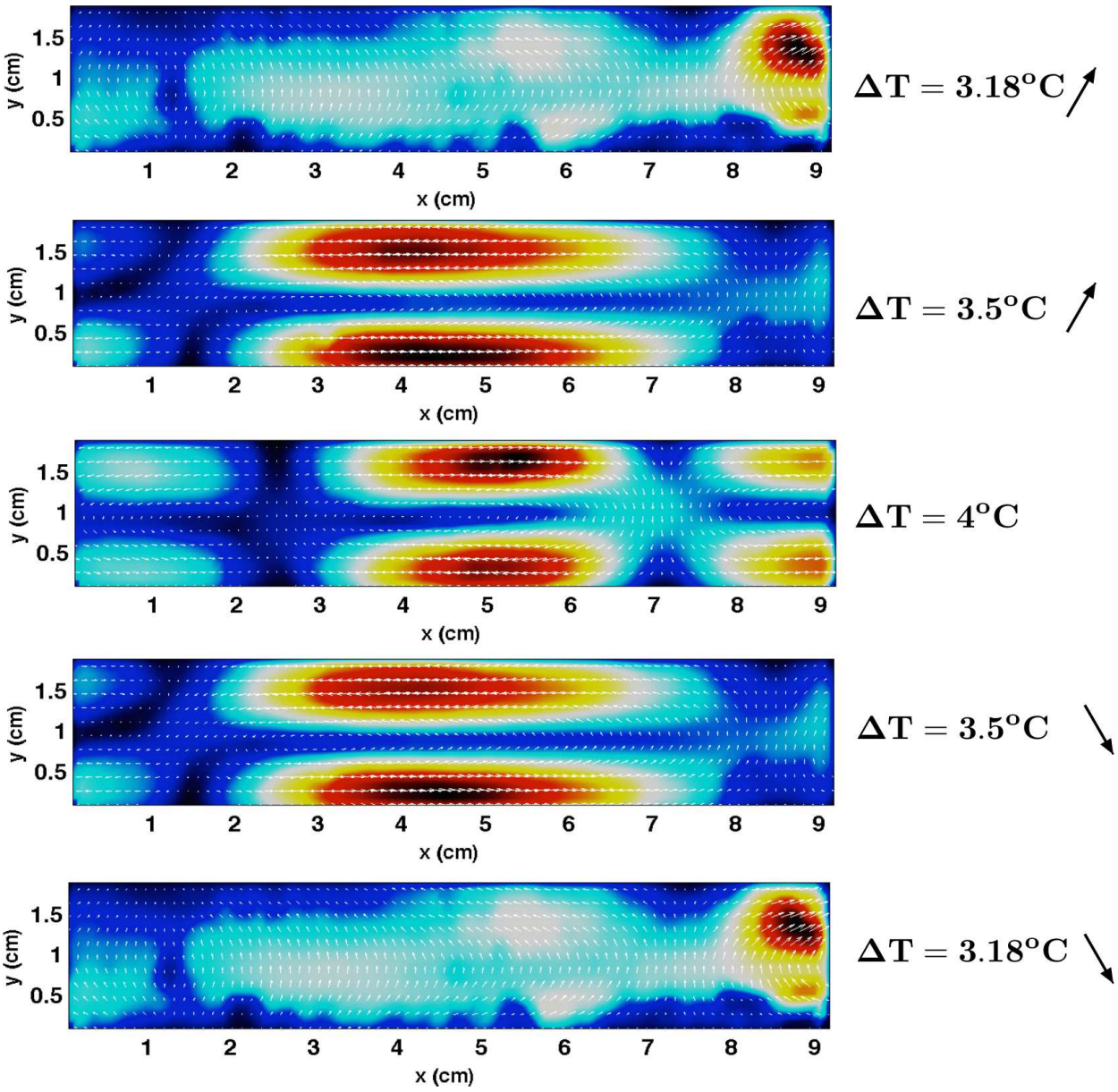

Figure 9: Evolution of the flow patterns corresponding to several values of the integral temperature difference ΔT indicated in the inserts. The up/down arrows indicate the increasing/decreasing branch of the heating ramp. The false colour map refers to the absolute value of the flow velocity. A 0.08% Carbopol® solution was used and the onset of the Rayleigh-Bénard convection corresponds to $\Delta T_c = 2.58^oC$.

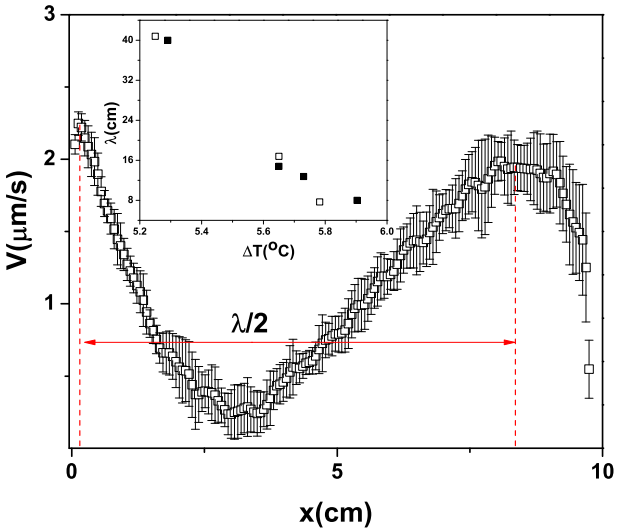

Figure 10: Time averaged longitudinal profile of the absolute value of the flow velocity measured at $z = H/2$ with a 0.075% Carbopol® solution at $\Delta T = 5.65^{o}C$. The error bars are defined by the root mean square deviation (rms) of the **DPIV** measured time series of longitudinal profile. The dependence of the size of the convective roll λ on the temperature difference ΔT is presented in the insert. The full/empty symbols refer to increasing/decreasing values of the heating power P.

states are reversible upon a decrease of the heating power (or temperature difference) which is a first indicator that, similarly to the Newtonian case, the transition to the Rayleigh-Bénard convection in the Carbopol® gel is a continuous one and exhibits no hysteresis. This qualitative similarity with the transition to convective states within a Newtonian fluid that deserves being studied in depth.

Measurements of the convective flow patterns such as the ones illustrated in Fig. 9 allows one to estimate the size of the stationary convection rolls corresponding to various heating powers P above the onset of the convection.

For this purpose, we monitor the profile of the absolute value of the flow velocity measured at half distance between the plates $z = H/2$, Fig. 10. The error bars in the measurement of the longitudinal profile of the absolute value of the velocity are defined by the root mean square deviation (rms) of a time series of roughly 100 velocity profiles.

In spite of the slight asymmetry of the roll pattern already noted in connection to Fig. 9 one can roughly estimate a characteristic size λ of the rolls by monitoring the distance between two consecutive maxima of the longitudinal velocity profile, Fig. 10. The dependence of the estimates of the characteristic roll size on the temperature difference between plates is presented in the insert of Fig. 10. Unfortunately, the size of the rolls could not be measured very close to the onset of the Rayleigh-Bénard convection as half of the roll size exceeds the size of the field of view of the digital camera.

In spite of this instrumental limitation it can be observed, however, that above the onset of the instability the size of the rolls decreases progressively which qualitatively agrees with theoretical predictions for the Newtonian case, Kramer and Riecke (1985). It is also notable that, consistently with the flow fields presented in Fig. 9, the size of the rolls is reproducible upon increasing/decreasing heat flux which reinforces once more the statement that the transition to convective states in the Carbopol® gel is supercritical.

Integral measurements of the dependence of the temperature difference between plates ΔT performed for six values of the Carbopol® concentration and for both increasing (the full symbols) and decreasing (the empty symbols) values of the heating power P are presented in Fig. 11.

For each value of the Carbopol® concentration a linear conductive part of the dependence is observed below a critical heating power P_c. The slopes of these linear dependencies are independent on the polymer concentration (see the full line in Fig. 11) indicating that the polymer addition does not significantly alter the thermal conductivity of the aqueous solutions. This result is fully consistent with direct measurements of the thermal conductivity coefficient κ

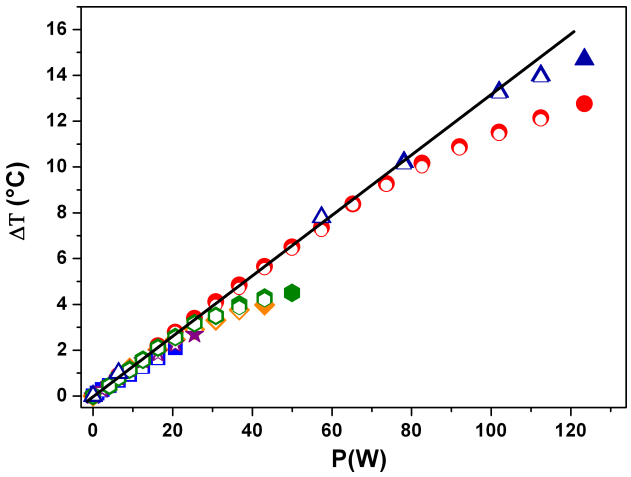

Figure 11: Dependence of temperature gradient on the heat flux for six values of the Carbopol concentration: (△, ▲) - $c = 0.11\%wt$, (○, ●) - $c = 0.1\%wt$, (⬠, ⬠) - $c = 0.08\%wt$, (⧫, ◇) - $c = 0.075\%wt$, (⋆, ✶) - $c = 0.06\%wt$, (□, ■) - $c = 0.05\%wt$. The full/empty symbols refer to increasing/decreasing heat flux. The full line is a linear fit.

$\mathbf{c}(\%\mathbf{wt})$	$\mathbf{\Delta T_c}(^{\mathbf{o}}\mathbf{C})$	$\mathbf{P_c}(\mathbf{W})$	$\mathbf{Y_c}$	$\mathbf{Ra_c}$
0.05	0.67	12.49	0.27	973.4
0.06	1	15.81	5.25	25.7
0.075	2.02	17.85	6.98	15.9
0.08	2.58	20.65	6.48	8.5
0.1	8.38	63.75	3.49	3.2
0.115	13.27	102	3.16	1.7

Table 2: Onset values of the relevant physical parameters.

performed for each solution separately and presented in Tab. 1.

Beyond the onset P_c, the dependence of the temperature difference between plates on the heating power becomes sub-linear and a convective regime is observed.

For clarity reasons and in order to facilitate the comparison of our results with the experiments by others, we list in Tab. 2 the parameters corresponding to the onset of the Rayleigh-Bénard convection for each of the Carbopol® solutions we have investigated.

Regardless the yield stress of the Cabopol® solution, sthe transition from a conductive to a convective regime is reversible upon increasing/decreasing values of the heating power and a strong qualitative similarity of these integral measurements to the similar ones performed with a Newtonian fluid and discussed in Sec. 3.1 is observed.

To gain a deeper insight into the nature of the bifurcation towards convective states within the Carbopol® solutions we present the same data in terms of the reduced variables ΔT_r, P_r. The dependence of the reduced temperature ΔT_r on the control parameter P_r for each Carbopol® solution is presented in Fig. 12 (a).

Above the onset of the bifurcation the reduced temperature ΔT_r scales linearly with the control parameter and this result is, as in the Newtonian case, typical for a super-critical bifurcation.

This fundamentally important conclusion on the nature of the bifurcation towards convective states is reinforced by the local measurements of the convective amplitude V presented in Fig. 12(b). Indeed, above the onset the bifurcation, the amplitude data can be well fitted by the Landau prediction for a super-critical bifurcation. The smearing of the transition data observed near the onset indicates that the bifurcation is an imperfect one.

Measurements of the slopes $\frac{\Delta Tr}{P_r}$ of the measurements presented in Fig. 12 **(a)** for various values of the yield stress τ_y are presented in Fig. 13. The error bars are defined by the error of the linear fitting functions presented as full

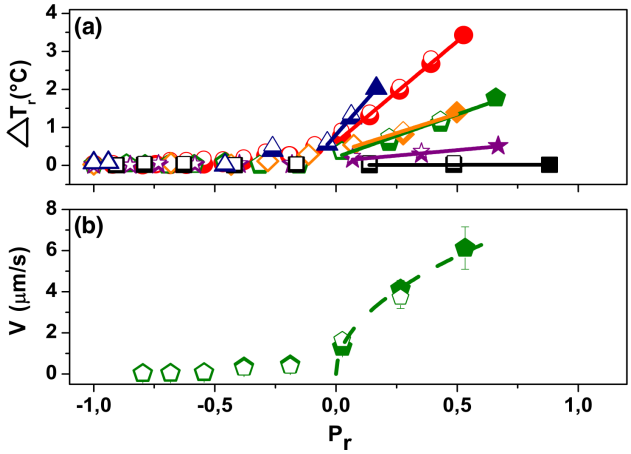

Figure 12: **(a)** Dependence of the reduced temperature T_r on the reduced power P_r for various Carbopol concentrations, see Fig. 11. The full lines are linear fitting functions. **(b)** Dependence the **DPIV** measured amplitude of the convection pattern V on the reduced power P_r. The dotted line is a square root fit function according to the Landau theory.

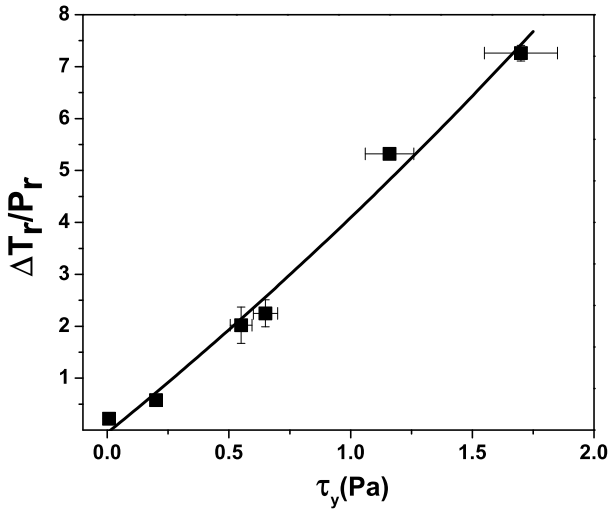

Figure 13: Dependence of the slopes $\frac{\Delta T_r}{P_r}$ of the measurements presented in Fig. 12 **(a)** on the yield stress τ_y of the Carbopol® solutions. The full line is an exponential fit.

lines in Fig. 12 **(a)**. An exponential scaling of these slopes with the yield stress of the fluid is found experimentally, $\frac{\Delta Tr}{P_r} \propto e^{\frac{\tau_y}{6.15}}$.

Thus, a gradual increase of the yield stress of the solution translates into a significant increase of the critical temperature difference that needs to be created between to destabilise the flow which explains the difficulty of observing and characterising the Rayleigh-Bénard convection in yield stress fluids.

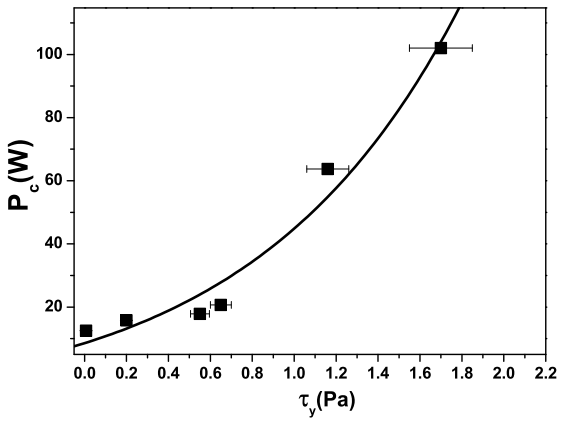

Figure 14: Dependence of the critical heating power P_c corresponding to the onset of the Rayleigh-Bénard convection on the yield stress τ_y of the Carbopol® solution. The line is an exponential fit.

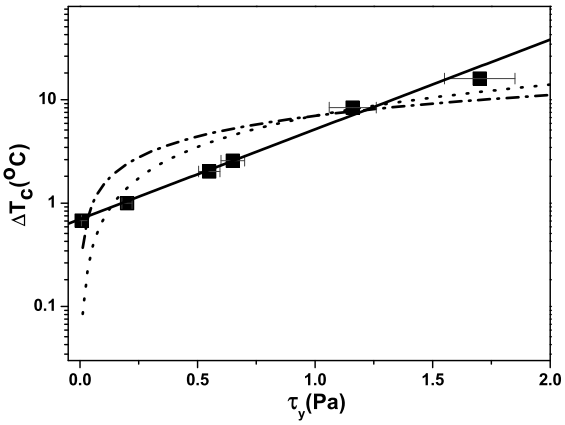

Figure 15: Dependence of the critical temperature difference between the plates corresponding to the he onset of the Rayleigh-Bénard convection ΔT_c on the yield stress (full symbols) and on the apparent yield stress (empty symbols) of the Carbopol® solution. The full lines are exponential fitting functions (see text). The dash-dotted line is the scaling proposed in Ref. Balmforth and Rust (2009), $\Delta T_c \propto \tau_y^{2/3}$. The dotted line is the experimentally found scaling in Ref. Darbouli et al. (2013), $\Delta T_c \propto \tau_y$.

We focus in the following on the dependence of the critical onset parameters (P_c, ΔT_c) on the yield stress of the solution. The dependence of the critical heating power P_c on the yield stress is presented in Fig. 14. According

to these measurements, the heating power needed to trigger convective states within the Carbopol® gel increases exponentially with its yield stress (the full line in Fig. 14): $P_c \propto e^{\frac{\tau_y}{0.97}}$.

A similar yield stress dependence of the critical temperature difference between the plates ΔT_c can be observed in Fig. 15: $\Delta T_c \propto e^{\frac{\tau_y}{0.5}}$.

These two experimental findings clearly highlight the practical difficulty of carrying on reliable Rayleigh-Bénard experiments with yield stress fluids which, in turn, may explain the very limited amount of reliable experimental data existing in the literature. An exponential increase of both the critical value of the heating power P_c and the critical temperature difference ΔT_c between the plates seriously limits the range of yield stresses that can be practically explored due to the difficulty in preventing strong thermal expansion effects that would practically lead to a mechanical breakdown of the convection cell. It is apparent from the exponential scaling laws of both P_c and ΔT_c that, with this experimental system, detecting the Rayleigh-Bénard convection in viscoplastic fluids with the yield stress significantly larger than unity becomes practically a challenging task.

The measurements of the critical physical parameters $\Delta T_c, P_c$ corresponding to the onset of the convection as a function of the yield stress of the Carbopol® solutions allows one to assess the degree of applicability of the onset conditions expressed by Eq's. 2, 3.

For this purpose, we focus on the dependencies of the slip critical yield number Y_c and the critical Rayleigh number Ra_c on the yield stress τ_y of the Carbopol® solution, Fig. 16.

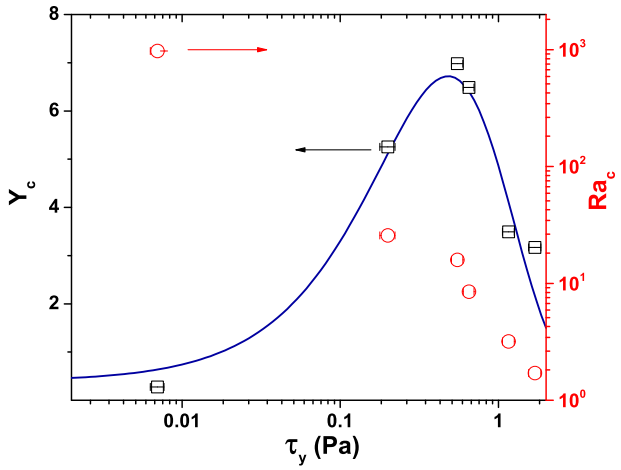

Figure 16: Dependence of the critical yield number Y_c (squares, bottom-left axis) and of the critical Rayleigh number Ra_c (circles, bottom-right axes) on the yield stress τ_y.

The critical Rayleigh number defined by Eq. 2 depends strongly on the yield stress of the fluid spanning nearly three decades as the concentration c of the Carbopol® solution is varied. This can be explained by the strong variation of the critical shear rate $\dot{\gamma}_c$ corresponding to the solid-fluid transition (see Fig. 1) on the yield stress. On the other hand, corresponding to the onset of the instability, the critical yield number Y_c defined by Eq. 3 has values of order of unity. Based on these data one can conclude that, unlike in the case of a Newtonian fluid which loses its stability towards convective states at well defined Rayleigh number (which does not depend on the viscosity), the onset of convection of the yield stress fluid is characterised by the yield number. This conclusion comes into a good agreement with the experimental findings of Darbouli and his coworkers, Darbouli et al. (2013).

A phenomenon typically associated with a super-critical bifurcation in pattern forming systems is the so called *critical slowing down* phenomenon. The critical slowing down phenomenon observed around the onset of a supercritical bifurcation manifests itself through an abrupt increase of the duration t_c of the dynamical transients as one approaches the criticality following a power law dependence $t_c \propto |P - Pc|^{-\alpha}$ where the scaling exponent α is typically of order of unity, Cross and Hohenberg (1993); Bodenschatz et al. (2000); Behringer and Ahlers (1977).

To probe the emergence of the critical slowing down phenomenon and characterise its main features in relation to the rheological properties of the solutions, we monitor the dependence of the characteristic times t_d, t_c (see Fig. 4(b)

and the discussion in Sec. 2.2) needed for the system to reach a state of thermal equilibrium on the heating power P. Measurements of the slowing down time t_c performed with a 0.075% Carbopol® solution are presented in Fig. 17. The error bars are defined here by the error of the nonlinear fittings of the temperature time series (the full line in Fig. 4(b)) by the Eq. 5.

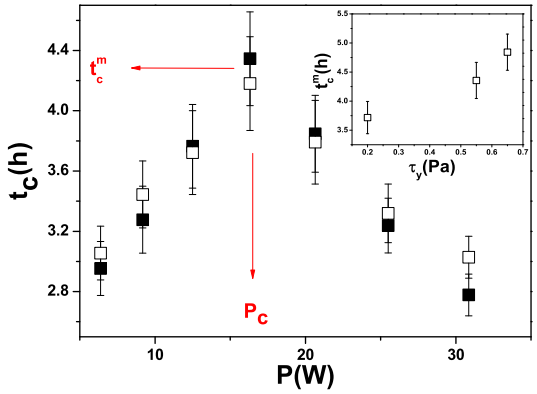

Figure 17: Dependence of the slowing down time t_c on the heating power P. A 0.075% Carbopol® solution was used. The full/empty symbols refer to increasing/decreasing heating powers. The insert presents the dependence of the critical slowing down time t_c^m on the yield stress τ_y of the Carbopol® solution. The full line is a linear fit.

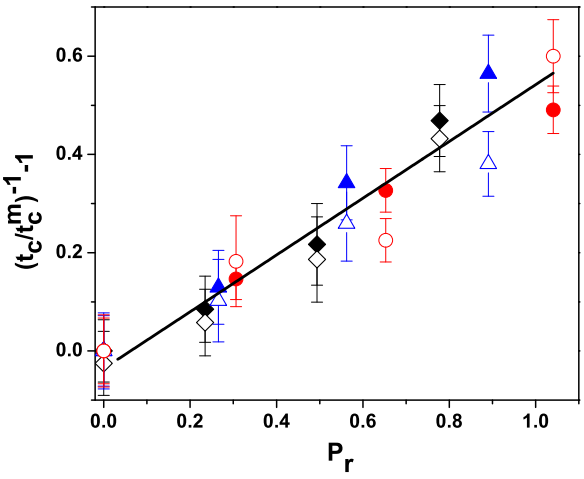

Figure 18: Dependence of the inverse scaled slowing down time on the heating reduced control parameter P_r for various Carbopol® solutions: (○, ●) - $c = 0.06\%$, (△, ▲) - $c = 0.075\%$, (◆, ◇) - $c = 0.08\%$. The full/empty symbols refer to increasing/decreasing values of the heating power P. The full line is a linear fit $\left(\frac{t_c}{t_c^m}\right)^{-1} - 1 = 0.56(\pm 0.15)P_r$.

The characteristic slowing down time t_c reaches a maximum corresponding to the onset of P_c of convection and the critical slowing down is observed. These measurements as well are reversible upon increasing/decreasing heating powers. The critical slowing down time t_c^m increases more or less linearly with the yield stress of the fluid (the insert in Fig. 17).

The characteristic times t_c measured for various Carbopol® solutions follow a universal dependence on the reduced heating powers P_r when normalised by the critical slowing down time, Fig. 18, and scale linearly with the reduced control parameter P_r. These findings are in a good agreement with previous theoretical predictions Wesfreid et al. (1978) and experimental results obtained for a Newtonian fluid, Behringer and Ahlers (1977) indicating once more a nearly one to one similarity with the Newtonian case.

To conclude this section, the main message of our experiments that the Rayleigh-Bénard convection can be triggered in Carbopol® solutions with a yield stress covering a broad range and, regardless the value of the yield stress, the transition to convective states can be unequivocally identified with a supercritical bifurcation.

We compare in the next section the experimental findings presented above with both theoretical predictions and experiments by others.

3.3. Comparison of our findings with theoretical predictions and experiments by others

As already pointed in the Introduction (Sec. 1) there exists a limited body of literature concerning the Rayleigh-Bénard convection in yield stress fluids, which will inherently limit the extent of the discussion below. In contrast to the linear stability analysis performed within the framework of the Bingham model by Zhang and her coworkers in Ref. Zhang et al. (2006) which demonstrates that the system is linearly stable, we do observe a transition towards convective states within various Carbopol® solutions exhibiting a clear yield stress behavior. This may imply that either the linear stability analysis or the Bingham rheological picture (or both) employed in Ref. Zhang et al. (2006) can not predict the loss of hydrodynamic stability within the Carbopol® gels we have investigated.

The weakly nonlinear stability analysis performed by Balmforth and Rust Balmforth and Rust (2009) confirms this point showing that convective states may be triggered within a Carbopol® gel if a sufficiently large perturbation

is applied onto the system. The magnitude of this perturbation was found to scale as $\tau_y^{2/3}$ with the yield stress of the fluid. In contrast to our experimental findings, the weakly non linear analysis performed within the framework of a regularised Bingham model predicts a subcritical bifurcation. This effect is related to the presence of a strong shear thinning effect. By varying the Carbopol® concentration we have decreased the power law index n of the solutions down to $n \approx 0.45$ (see the insert in Fig. 2) but, within the accuracy and resolution of our measurements, we have observed no clear sign of a supercritical bifurcation. We also note that, regardless the yield stress, the transition to convective states was observed in our experiments without intentionally perturbing the system (neither mechanically nor thermally).

Previous experiments on the Rayleigh-Bénard convection in Carbopol® did not identify unequivocally a subcritical bifurcation either. Darbouli and his coworkers have identified some sort of irreversibility during some of their measurements of the temperature difference between plates but did not identify it in most of the other and a correlation of this effect with a physical property of the gels is not obvious, Darbouli et al. (2013).

Irreversible (upon increasing/decreasing heating powers) measurements of the temperature difference between plates may also be related to experimental artefacts.

A first source of experimental artefacts may come from not properly accounting for the emergence of the critical slowing down phenomenon. Indeed, as illustrated in Fig. 17 the time needed for the system to reach a steady state increases drastically as one approaches the critical point and taking the temperature point after the same fixed time interval regardless the distance from the onset (the value of the reduced control parameter P_r) may translate into the irreproducibility of the data around the onset which might be mistakingly interpreted as a hysteresis and lead to an incorrect conclusion on the physical nature of the bifurcation. During our measurements, such artefacts have been carefully avoided by always taking the temperature measurements at times larger than the duration of the transients, $t > t_d + t_c$ (see Fig. 4 and the discussion in Sec. 2.2).

A second source of experimental artefacts may be related to the lateral boundary conditions of the convection cell. As shown theoretically by Brown and Stewartson, an imperfect insulation of the walls of a cylindrical Rayleigh-Bénard cell may induce a subcritical bifurcation, Brown and Setwartson (1978); Brown and Stewartson (1979).

Our experiments have been conducted in a rectangular convection cell with fairly good insulating acrylic made lateral walls. Also, the longitudinal to vertical aspect ratio of our cell is quite large, $L/H = 19.3$.

It is interesting to compare the experimentally found scalings illustrated in Figs. 14, 15 with the existing theoretical predictions and the experimental results by others. The detailed weakly nonlinear stability analysis presented by Balmforth and Rust indicates that the magnitude of the perturbation able to trigger the convection scales as $\Delta T_c \propto \tau_y^{2/3}$ (the dash-dotted line in Fig. 15). The experiments by Darbouli and his coworkers suggest a linear scaling of ΔT_c with the yield stress. The experimentally found scaling of the critical temperature difference ΔT_c with the yield stress illustrated in Fig. 15 differs from both the theoretical predictions and the results by Darbouli and his coworkers. The discrepancy of the experimental scaling result with the weakly nonlinear analysis results may be related to the rheological framework Balmforth and Rust have considered, namely its limited ability to describe the solid-fluid transition in a Carbopol® gel. As pointed out for the first time in Ref. Putz and Burghelea (2009) and illustrated in Fig. 1, the rheological behaviour of the gel around its yield point is more complicated than the Bingham (or Herschel-Bulkley) picture. To probe the relevance of the rheological yielding scenario illustrated in Fig. 1 to the convection experiments described above, we turn our attention to measurements of the velocity gradients performed within a 0.08% Carbopol® solution slightly above the onset of the Rayleigh-Bénard instability, Fig. 19.

Due to the smallness of the velocity gradients illustrated in Fig. 19 it is obvious that the rheological regime relevant around the convective onset is the intermediate and irreversible solid-fluid regime visible in Fig. 1 in a range of applied stresses right above the elastic solid regime ($\dot{\gamma} = ct.$). Within this deformation regime, the rheological response of the material departs significantly from the Bingham, Herschel-Bulkley models and their regularised versions.

This provides a plausible explanation for the partial disagreement between our experimental findings and previous theoretical works.

4. Conclusions, outlook

A systematic experimental investigation of the Rayleigh-Bénard convection in a yield stress fluid is presented by combined integral measurements of the temperature gradient between the plates and local measurements of the amplitude of the flow patterns.

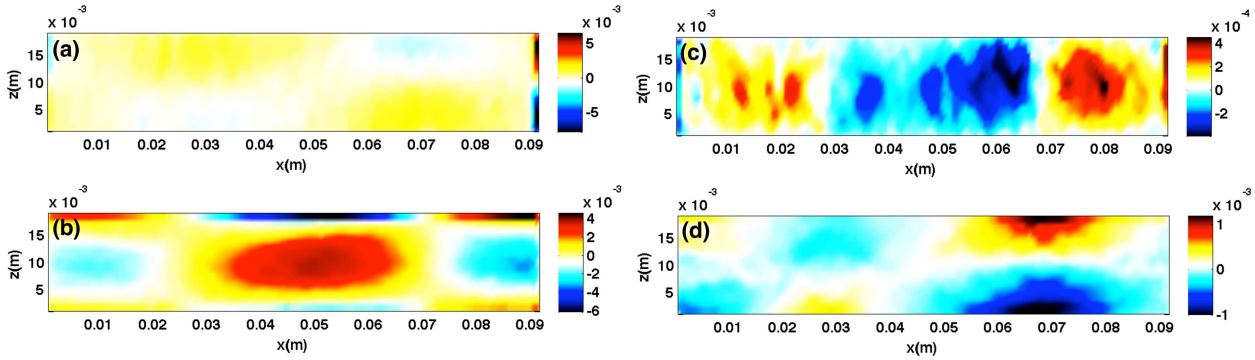

Figure 19: **DPIV** measured velocity gradients: **(a)** $\frac{\partial V_x}{\partial x}$ **(b)** $\frac{\partial V_x}{\partial z}$ **(c)** $\frac{\partial V_z}{\partial x}$ **(d)** $\frac{\partial V_z}{\partial z}$. A 0.08% Carbopol® solution was used and the temperature difference between plates was $\Delta T = 4^o\ C$.

The reliability of the experimental system and measurement techniques has been demonstrated by characterising the Rayleigh-Bénard convection in a Newtonian fluid. Thus, we have found a transition to convective states in a Glyecerin solution corresponding to values of the critical Rayleigh number fairly close to the theoretical values. Besides that, we have clearly identified the bifurcation towards convective states as a super-critical one (see Figs. 6, 7) in a full agreement with both theoretical predictions and previous experimental studies.

Following exactly the same experimental procedure and data reduction strategy as for the validation experiments, the emergence and the physical features of Rayleigh-Bénard the convection have been investigated for six Carbopol® solutions with concentrations larger than the overlap concentration c^* (thus, each solution we have investigated exhibited both yield stress and shear thinning behaviour).

For each polymer concentration (yield stress) a clear transition to convective states is observed when the heating power exceeds a critical value P_c by both local **DPIV** measurements of the amplitude of the flow pattern and integral measurements of the temperature difference between plates. It is important to point out that, during our experiments, the instability was observed in the absence of an externally applied perturbation of a finite amplitude.

As compared to the Newtonian convective patterns, the rolls observed within Carbopol® solutions have a different topology. They are flatter near the boundaries indicating significant differences in the physical properties of the viscous (Newtonian) and viscoplastic boundary layers, Fig. 8.

The following features that unequivocally identify the transition to the Rayleigh-Bénard convection in various Carbopol® gels as an imperfect (super-critical) bifurcation have been identified experimentally:

1. The dynamic states are reversible upon an increase/decrease of the control parameter, Figs. 11, 12.
2. Above the onset of the Rayleigh-Bénard convection the reduced temperature difference scales linearly with the reduced control parameter, Fig. 12 (a). The slopes of these linear dependencies decrease exponentially with the yield stress of the Carbopol® solution, Fig. 13.
3. A square root scaling as predicted by the Landau theory of the phase transitions is found for the locally measured amplitude of the convective pattern, Fig. 12 (b).
4. The transition to convective states within the Carbopol® gels exhibits the critical slowing down phenomenon, Fig. 17, and the critical slowing down time t_c^m increases linearly with the yield stress τ_y of the Carbopol® solution. When normalised by the critical slowing down time, the data acquired for various Carbopol® solutions collapses onto the same master curve, Fig. 18 and the slope of this dependence is in an excellent agreement with previous measurements performed for Newtonian fluids, Behringer and Ahlers (1977).

As opposed to the case of Newtonian fluids where the onset of the Rayleigh-Bénard instability is described by a theoretically predicted value of the Rayleigh number Ra, the thermal convection in a Carbopol® gel occurs at values of the yield number Y of order of unity for the entire range of yield stresses we have explored, Fig. 16. Due to the strong dependence on the yield stress of the critical rate of shear $\dot{\gamma}_c$ corresponding to the yielding transition, the plastic critical Rayleigh number Ra_c varies three orders as the yield stress is varied. These results indicate that the onset of

the instability is related to a energy balance criterion involving the elastic energy associated to the gel microstructure, rather than a classical force balance criterion involving the viscous forces. This finding agrees qualitatively well with previous experimental results, Davaille et al. (2013); Darbouli et al. (2013), although the values of the yield number are found significantly larger.

The comparison of our experimental results with existing theoretical predictions and previous experimental results reveals a number of discrepancies. In spite of the clear shear thinning behaviour of the fluids, the continuous nature of the bifurcation is at odds with the results of the weakly nonlinear stability analysis performed within the framework of the Bingham model, Balmforth and Rust (2009). A comparison of this result with the experimental results reported by Darbouli and his coworkers in Ref. Darbouli et al. (2013) is more difficult to make as they observe both reversible (consistent with a supercritical bifurcation) and irreversible behaviour (hysteresis, consistent with a subcritical bifurcation) and a correlation of their observations with the rheological properties of the solutions is not straightforward as it may due to various factors such as the instrumental resolution, the experimental protocol and the boundary conditions etc. . From a quantitative point of view, an agreement with the previous experiments was not found either: in spite of the significantly lower yield stress of the solutions (with concentrations of Carbopol® comparable to ours) the critical temperature difference ΔT_c at which the onset of the instability is detected is found systematically larger in Ref. Darbouli et al. (2013).

The measurements of the velocity gradients above the onset of the instability presented in Fig. 19 confirm that the Rayleigh-Bénard instability and the solid-fluid transition in a Carbopol® gel are coupled. Thus, future theoretical and/or numerical studies of the onset of the instability should involve rheological models that can properly account for the coexistence between solid (unyielded) and fluid (yielded) material elements rather than the classical rheological pictures.

Acknowledgments

The work was supported by the grant *"ANR ThIM"* provided by the *"Agence Nationale de la Recherche"*, France.

We are deeply indebted to Mr. Christophe Le Bozec for his help in setting up the experimental system and interfacing the temperature measurements.

We gratefully acknowledge the technical support of Thermo Fisher Scientific, Karlsruhe, Germany for the calibration of the nano-torque module installed on the Mars III rheometer.

References

Balmforth, N. J., Rust, A. C., 2009. Weakly nonlinear viscoplastic convection. Journal of Non-Newtonian Fluid Mechanics 158 (1-3), 36 – 45.

Behringer, R., Ahlers, G., 1977. Heat transport and critical slowing down near the Rayleigh-Bénard instability in cylindrical containers. Physics Letters A 62 (5), 329 – 331.
URL http://www.sciencedirect.com/science/article/pii/0375960177904315

Bertola, V., 2009. Wicking with a yield stress fluid. Journal of Physics: Condensed Matter 21 (3), 035107.
URL http://stacks.iop.org/0953-8984/21/i=3/a=035107

Bodenschatz, E., Pesch, W., Ahlers, G., 2000. Recent developments in Rayleigh-Bénard convection. Annual Review of Fluid Mechanics 32 (1), 709–778.

Brown, S., Stewartson, K., 1979. On finite amplitude bénard convection in a cylindrical container. part ii. SIAM Journal on Applied Mathematics 36 (3), 573–586.
URL http://epubs.siam.org/doi/abs/10.1137/0136041

Brown, S. N., Setwartson, K., 1978. On finite amplitude benard convection in a cylindrical container. Proc. R. Soc. Lond. A 360, 455–469.

Chandrasekhar, S., 1961. Hydrodynamic and hydromagnetic stability. Oxford : Clarendon press.

Cross, M. C., Hohenberg, P. C., Jul 1993. Pattern formation outside of equilibrium. Rev. Mod. Phys. 65, 851–1112.
URL http://link.aps.org/doi/10.1103/RevModPhys.65.851

Darbouli, M., Metivier, C., Piau, J.-M., Magnin, A., Abdelali, A., 2013. Rayleigh-Bénard convection for viscoplastic fluids. Physics of Fluids 25 (2), 023101.
URL http://link.aip.org/link/?PHF/25/023101/1

Davaille, A., Gueslin, B., Massmeyer, A., Giuseppe, E. D., 2013. Thermal instabilities in a yield stress fluid: Existence and morphology. Journal of Non-Newtonian Fluid Mechanics 193 (0), 144 – 153, <ce:title>Viscoplastic Fluids: From Theory to Application</ce:title>.
URL http://www.sciencedirect.com/science/article/pii/S0377025712002261

Dubois, M., Bergé, P., 3 1978. Experimental study of the velocity field in Rayleigh-Bénard convection. Journal of Fluid Mechanics 85, 641–653.

Frigaard, I., Howison, S., Sobey, I., 1994. On the stability of poiseuille flow of a bingham fluid. J. Fluid Mech. 263, 133–150.

Griggs, D. T., 1939. A theory of mountain-building. American Journal of Science 237, 611–650.

Herschel, W., Bulkley, T., 1926. Measurement of consistency as applied to rubber-benzene solutions. Am. Soc. Test Proc. 26(2), 621âĂŽĂĎÃń633.
Kim, J.-Y., Song, J.-Y., Lee, E.-J., Park, S.-K., 2003. Rheological propertoies and microstructures of carbopol gel network system. Colloid Polym. Sci. 281 (7), 614–623.
Koschmieder, E. L., 1993. Bénard Cells and Taylor vortices. Cambridge University Press.
Kramer, L., Riecke, H., 1985. Wavelength selection in Rayleigh-Bénard convection. Zeitschrift fÃijr Physik B Condensed Matter 59 (3), 245–251. URL http://dx.doi.org/10.1007/BF01307426
Lamsaadi, M., Naomi, M., Hasnaoui, M., 2005. Natural convection of non-Newtonian power law fluids in a shallow horizontal rectangular cavity uniformly heated from below. Heat and Mass Transfer 41, 239–249.
Landry, M. P., Frigaard, I. A., Martinez, D. M., 2006. Stability and instability of taylor - couette flows of a bingham fluid. Journal of Fluid Mechanics 560, 321–353.
Le Bars, M., Davaille, A., 2004. Whole layer convection in a heterogeneous planetary mantle. Journal of Geophysical Research 109, 23.
Meinesz, F. A. V., 1947. Major tectonic phenomena and the hypothesis of convection currents in the earth. Quarterly Journal of the Geological Society 103 (1-4), 191–207,NP.
Metivier, C., Nouar, C., Brancher, J.-P., 2005. Linear stability involving the Bingham model when the yield stress approaches zero. Physics of Fluids 17 (10), 104106.
Newell, A. C., Whitehead, J. A., 8 1969. Finite bandwidth, finite amplitude convection. Journal of Fluid Mechanics 38, 279–303.
Orowan, E., 1965. Convection in a non-newtonian mantle, continental drift, and mountain building. Philosophical Transactions of the Royal Society of London. Series A, Mathematical and Physical Sciences 258 (1088), 284–313.
Park, H., Park, K., 2004. Rayleigh-Bénard convection of viscoelastic fluids in arbitrary finite domains. International Journal of Heat and Mass Transfer 47 (10-11), 2251 – 2259.
Park, H., Ryu, D., 2001. Rayleigh-Bénard convection of viscoelastic fluids in finite domains. Journal of Non-Newtonian Fluid Mechanics 98 (2-3), 169 – 184.
Piau, J., 2007. Carbopol gels: Elastoviscoplastic and slippery glasses made of individual swollen sponges: Meso- and macroscopic properties, constitutive equations and scaling laws. Journal of Non-Newtonian Fluid Mechanics 144 (1), 1 – 29.
Putz, A. M. V., Burghelea, T. I., 2009. The solid-fluid transition in a yield stress shear thinning physical gel. Rheol Acta 48, 673–689.
Raffel, M., Willert, C. E., Wereley, S. T., Kompenhans, J., September 2007. Particle Image Velocimetry: A Practical Guide (Experimental Fluid Mechanics). Springer; 2nd edition.
Scarano, F., Rhiethmuller, M. L., 2001. Advances in iterative multigrid piv image processing. Exp. Fluids 29.
Segel, L. A., 7 1969. Distant side-walls cause slow amplitude modulation of cellular convection. Journal of Fluid Mechanics 38, 203–224.
Turan, O., Chakraborty, N., Poole, R. J., 2012. Laminar Rayleigh-Bénard convection of yield stress fluids in a square enclosure. Journal of Non-Newtonian Fluid Mechanics 171-172 (0), 83 – 96.
Uhlherr, P. H. T., Guo, J., Tiu, C., Zhang, X. M., Zhou, J. Z. Q., Fang, T. N., 2005. The shear-induced solid-liquid transition in yield stress materials with chemically different structures. J. Non-Newtonian Fluid Mech. 125, 101–119.
Weber, E., Moyers-GonzÃąlez, M., Burghelea, T. I., 2012. Thermorheological properties of a carbopol gel under shear. Journal of Non-Newtonian Fluid Mechanics 183âĂŞ184 (0), 14 – 24.
URL http://www.sciencedirect.com/science/article/pii/S0377025712001322
Wesfreid, J., Pomeau, Y., Dubois, M., Normand, C., Berge, P., 1978. Critical effects in Rayleigh-Bénard convection. J. Phys. France 39 (7), 725–731.
Zhang, J., Vola, D., Frigaard, I. A., 2006. Yield stress effects on Rayleigh-Bénard convection. J. Fluid Mech 566, 389.